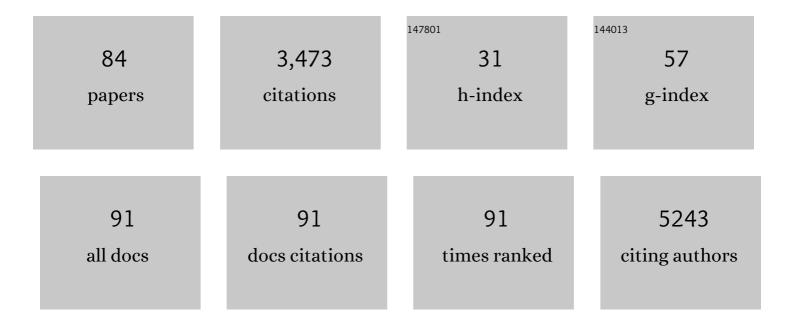
Juan C HernÃ;ndez-Garrido

List of Publications by Year in descending order

Source: https://exaly.com/author-pdf/1676501/publications.pdf

Version: 2024-02-01



#	Article	IF	CITATIONS
1	Honeycomb monolithic design to enhance the performance of Ni-based catalysts for dry reforming of methane. Catalysis Today, 2022, 383, 226-235.	4.4	8
2	Selective semi-hydrogenation of internal alkynes catalyzed by Pd–CaCO3 clusters. Journal of Catalysis, 2022, 408, 43-55.	6.2	29
3	Low-Temperature Growth of Reactive Pyrochlore Nanostructures on Zirconia-Supported Ceria: Implications for Improved Catalytic Behavior. ACS Applied Nano Materials, 2022, 5, 6316-6326.	5.0	2
4	3D-printing of metallic honeycomb monoliths as a doorway to a new generation of catalytic devices: the Ni-based catalysts in methane dry reforming showcase. Catalysis Communications, 2021, 148, 106181.	3.3	28
5	Soluble/MOF-Supported Palladium Single Atoms Catalyze the Ligand-, Additive-, and Solvent-Free Aerobic Oxidation of Benzyl Alcohols to Benzoic Acids. Journal of the American Chemical Society, 2021, 143, 2581-2592.	13.7	74
6	Regioirregular and catalytic Mizoroki–Heck reactions. Nature Catalysis, 2021, 4, 293-303.	34.4	42
7	In-depth structural and analytical study of the washcoating layer of a Mn-Cu monolithic catalyst using STEM-FIB, EDX and EELS. Insights into stability under working conditions. Applied Surface Science, 2021, 563, 150318.	6.1	2
8	Ultrathin Washcoat and Very Low Loading Monolithic Catalyst with Outstanding Activity and Stability in Dry Reforming of Methane. Nanomaterials, 2020, 10, 445.	4.1	8
9	The Role of Goldâ€Alumina Template in the Electrochemical Deposition of CeO 2 Nanotubes. Particle and Particle Systems Characterization, 2019, 36, 1900168.	2.3	3
10	HAADF-STEM Electron Tomography in Catalysis Research. Topics in Catalysis, 2019, 62, 808-821.	2.8	16
11	C-doped anatase TiO2: Adsorption kinetics and photocatalytic degradation of methylene blue and phenol, and correlations with DFT estimations. Journal of Colloid and Interface Science, 2019, 547, 14-29.	9.4	87
12	An atomically efficient, highly stable and redox active Ce0.5Tb0.5Ox (3% mol.)/MgO catalyst for total oxidation of methane. Journal of Materials Chemistry A, 2019, 7, 8993-9003.	10.3	12
13	Sunlight photoactivity of rice husks-derived biogenic silica. Catalysis Today, 2019, 328, 125-135.	4.4	21
14	Base-Controlled Heck, Suzuki, and Sonogashira Reactions Catalyzed by Ligand-Free Platinum or Palladium Single Atom and Sub-Nanometer Clusters. Journal of the American Chemical Society, 2019, 141, 1928-1940.	13.7	107
15	Surface and redox characterization of new nanostructured ZrO ₂ @CeO ₂ systems with potential catalytic applications. Surface and Interface Analysis, 2018, 50, 1025-1029.	1.8	10
16	Synthesis of Densely Packaged, Ultrasmall Pt ⁰ ₂ Clusters within a Thioetherâ€Functionalized MOF: Catalytic Activity in Industrial Reactions at Low Temperature. Angewandte Chemie, 2018, 130, 6294-6299.	2.0	22
17	Synthesis of Densely Packaged, Ultrasmall Pt ⁰ ₂ Clusters within a Thioetherâ€Functionalized MOF: Catalytic Activity in Industrial Reactions at Low Temperature. Angewandte Chemie - International Edition, 2018, 57, 6186-6191.	13.8	115
18	Multicationic Sr4Mn3O10 mesostructures: molten salt synthesis, analytical electron microscopy study and reactivity. Materials Horizons, 2018, 5, 480-485.	12.2	5

#	Article	IF	CITATIONS
19	Low temperature prepared copper-iron mixed oxides for the selective CO oxidation in the presence of hydrogen. Applied Catalysis A: General, 2018, 552, 58-69.	4.3	23
20	Confined Pt ₁ ¹⁺ Water Clusters in a MOF Catalyze the Lowâ€Temperature Water–Gas Shift Reaction with both CO ₂ Oxygen Atoms Coming from Water. Angewandte Chemie - International Edition, 2018, 57, 17094-17099.	13.8	54
21	Exploring the Capability of HAADF-STEM Techniques to Characterize Graphene Distribution in Nanocomposites by Simulations. Journal of Nanomaterials, 2018, 2018, 1-12.	2.7	Ο
22	Confined Pt ₁ ¹⁺ Water Clusters in a MOF Catalyze the Lowâ€Temperature Water–Gas Shift Reaction with both CO ₂ Oxygen Atoms Coming from Water. Angewandte Chemie, 2018, 130, 17340-17345.	2.0	4
23	Synthesis of Supported Planar Iron Oxide Nanoparticles and Their Chemo- and Stereoselectivity for Hydrogenation of Alkynes. ACS Catalysis, 2017, 7, 3721-3729.	11.2	63
24	Intra-particle chemical homogeneity determining the exchange coupling in palladium-iron nanoparticles. Journal of Applied Physics, 2017, 121, 084302.	2.5	0
25	Improving the Redox Response Stability of Ceria-Zirconia Nanocatalysts under Harsh Temperature Conditions. Chemistry of Materials, 2017, 29, 9340-9350.	6.7	21
26	Highly stable ceria-zirconia-yttria supported Ni catalysts for syngas production by CO 2 reforming of methane. Applied Surface Science, 2017, 426, 864-873.	6.1	46
27	Critical Influence of Redox Pretreatments on the CO Oxidation Activity of BaFeO3â^`δ Perovskites: An in-Depth Atomic-Scale Analysis by Aberration-Corrected and in Situ Diffraction Techniques. ACS Catalysis, 2017, 7, 8653-8663.	11.2	13
28	Synthetic mimetics of the endogenous gastrointestinal nanomineral: Silent constructs that trap macromolecules for intracellular delivery. Nanomedicine: Nanotechnology, Biology, and Medicine, 2017, 13, 619-630.	3.3	17
29	A promoting effect of dilution of Pd sites due to gold surface segregation under reaction conditions on supported Pd–Au catalysts for the selective hydrogenation of 1,5-cyclooctadiene. Catalysis Today, 2016, 259, 213-221.	4.4	24
30	The impact of the chemical synthesis on the magnetic properties of intermetallic PdFe nanoparticles. Journal of Nanoparticle Research, 2015, 17, 1.	1.9	14
31	Comparative study of the catalytic performance and final surface structure of Co3O4/La-CeO2 washcoated ceramic and metallic honeycomb monoliths. Catalysis Today, 2015, 253, 190-198.	4.4	26
32	An endogenous nanomineral chaperones luminal antigen and peptidoglycan to intestinal immune cells. Nature Nanotechnology, 2015, 10, 361-369.	31.5	73
33	Direct formic acid fuel cells on Pd catalysts supported on hybrid TiO2-C materials. Applied Catalysis B: Environmental, 2015, 163, 167-178.	20.2	43
34	A novel CoOx/La-modified-CeO2 formulation for powdered and washcoated onto cordierite honeycomb catalysts with application in VOCs oxidation. Applied Catalysis B: Environmental, 2014, 144, 425-434.	20.2	67
35	Experimental evidences of the relationship between reducibility and micro- and nanostructure in commercial high surface area ceria. Applied Catalysis A: General, 2014, 479, 35-44.	4.3	13
36	One pot synthesis of cyclohexanone oxime from nitrobenzene using a bifunctional catalyst. Chemical Communications, 2014, 50, 1645-1647.	4.1	21

#	Article	IF	CITATIONS
37	Exploring the benefits of electron tomography to characterize the precise morphology of core–shell Au@Ag nanoparticles and its implications on their plasmonic properties. Nanoscale, 2014, 6, 12696-12702.	5.6	16
38	Speciation-controlled incipient wetness impregnation: A rational synthetic approach to prepare sub-nanosized and highly active ceria–zirconia supported gold catalysts. Journal of Catalysis, 2014, 318, 119-127.	6.2	20
39	High-Resolution Spectroscopy of Europium-Doped Ceria as a Tool To Correlate Structure and Catalytic Activity. Journal of Physical Chemistry C, 2014, 118, 23349-23360.	3.1	12
40	The promotional effect of Sn-beta zeolites on platinum for the selective hydrogenation of α,β-unsaturated aldehydes. Physical Chemistry Chemical Physics, 2013, 15, 12048.	2.8	32
41	Rational design of nanostructured, noble metal free, ceria–zirconia catalysts with outstanding low temperature oxygen storage capacity. Journal of Materials Chemistry A, 2013, 1, 4836.	10.3	42
42	Self-assembly of one-pot synthesized CexZr1â^'xO2–BaO•nAl2O3 nanocomposites promoted by site-selective doping of alumina with barium. Journal of Materials Chemistry A, 2013, 1, 3645.	10.3	12
43	2D and 3D characterization of a surfactant-synthesized TiO2–SiO2 mesoporous photocatalyst obtained at ambient temperature. Physical Chemistry Chemical Physics, 2013, 15, 2800.	2.8	26
44	Nanocrystalline carbon–TiO2 hybrid hollow spheres as possible electrodes for solar cells. Carbon, 2013, 53, 169-181.	10.3	32
45	Combined (S)TEM-FIB Insight into the Influence of the Preparation Method on the Final Surface Structure of a Co ₃ O ₄ /La-Modified-CeO ₂ Washcoated Monolithic Catalyst. Journal of Physical Chemistry C, 2013, 117, 13028-13036.	3.1	13
46	Suppression and enhancement of the ferromagnetic response in Fe-doped ZnO nanoparticles by calcination of organic nitrogen, phosphorus, and sulfur compounds. Journal of Nanoparticle Research, 2013, 15, 1.	1.9	3
47	Nanoconfinement of Ni clusters towards a high sintering resistance of steam methane reforming catalysts. Catalysis Science and Technology, 2012, 2, 2476.	4.1	20
48	Exceptional Activity for Methane Combustion over Modular Pd@CeO ₂ Subunits on Functionalized Al ₂ O ₃ . Science, 2012, 337, 713-717.	12.6	842
49	Biomass into chemicals: One-pot two- and three-step synthesis of quinoxalines from biomass-derived glycols and 1,2-dinitrobenzene derivatives using supported gold nanoparticles as catalysts. Journal of Catalysis, 2012, 292, 118-129.	6.2	70
50	Pd (1Âwt%)/LaMn0.4Fe0.6O3 Catalysts Supported Over Silica SBA-15: Effect of Perovskite Loading and Support Morphology on Methane Oxidation Activity and SO2 Tolerance. Topics in Catalysis, 2012, 55, 782-791.	2.8	9
51	Unknown Aspects of Self-Assembly of PbS Microscale Superstructures. ACS Nano, 2012, 6, 3800-3812.	14.6	92
52	Morphological Study of Nanoparticleâ^'Polymer Solar Cells Using High-Angle Annular Dark-Field Electron Tomography. Nano Letters, 2011, 11, 904-909.	9.1	76
53	Advanced Electron Microscopy Investigation of Ceria–Zirconiaâ€Based Catalysts. ChemCatChem, 2011, 3, 1015-1027.	3.7	16
54	The location of gold nanoparticles on titania: A study by high resolution aberration-corrected electron microscopy and 3D electron tomography. Catalysis Today, 2011, 160, 165-169.	4.4	38

#	Article	IF	CITATIONS
55	Exceptionally Active Singleâ€6ite Nanocluster Multifunctional Catalysts for Cascade Reactions. ChemCatChem, 2010, 2, 402-406.	3.7	19
56	Electron tomography of Illâ€V quantum dots using dark field 002 imaging conditions. Journal of Microscopy, 2010, 237, 148-154.	1.8	5
57	Using Highly Accurate 3D Nanometrology to Model the Optical Properties of Highly Irregular Nanoparticles: A Powerful Tool for Rational Design of Plasmonic Devices. Nano Letters, 2010, 10, 2097-2104.	9.1	54
58	Fabrication and characterization of TiN nanocomposite powders fabricated by DC arc-plasma method. Journal of Alloys and Compounds, 2010, 492, 685-690.	5.5	11
59	Nanostructural characterization and catalytic analysis of hybridized platinum/phthalocyanine nanocomposites. Microscopy (Oxford, England), 2009, 58, 289-294.	1.5	5
60	Probing Solid Catalysts under Operating Conditions: Electrons or Xâ€rays?. Angewandte Chemie - International Edition, 2009, 48, 3904-3907.	13.8	39
61	3 D Characterization of Gold Nanoparticles Supported on Heavy Metal Oxide Catalysts by HAADF‧TEM Electron Tomography. Angewandte Chemie - International Edition, 2009, 48, 5313-5315.	13.8	72
62	A General Strategy for the Design of New Solid Catalysts for Environmentally Benign Conversions. Topics in Catalysis, 2009, 52, 1630-1639.	2.8	31
63	TEM, HRTEM, electron holography and electron tomography studies of γ′ and γ″ nanoparticles in Inconel 718 superalloy. Journal of Microscopy, 2009, 236, 149-157.	1.8	26
64	Fabrication and characterization of TiN–Ag nano-dice. Micron, 2009, 40, 308-312.	2.2	23
65	3D imaging of nanomaterials by discrete tomography. Ultramicroscopy, 2009, 109, 730-740.	1.9	255
66	Comparative study of the reducibility under H2 and CO of two thermally aged Ce0.62Zr0.38O2 mixed oxide samples. Catalysis Today, 2009, 141, 409-414.	4.4	27
67	Scanning Transmission Electron Microscopy Investigation of Differences in the High Temperature Redox Deactivation Behavior of CePrOx Particles Supported on Modified Alumina. Chemistry of Materials, 2009, 21, 1035-1045.	6.7	18
68	Nanoporous oxidic solids: the confluence of heterogeneous and homogeneous catalysis. Physical Chemistry Chemical Physics, 2009, 11, 2799.	2.8	63
69	Morphology of SBA-15-directed by association processes and surface energies. Physical Chemistry Chemical Physics, 2009, 11, 10973.	2.8	34
70	Developments in Techniques and Algorithms for Materials-Based Electron Tomography. Microscopy and Microanalysis, 2009, 15, 40-41.	0.4	0
71	Equilibrium and Kinetic Properties of Cu ^{II} Cyclophane Complexes: The Effect of Changes in the Macrocyclic Cavity Caused by Changes in the Substitution at the Aromatic Ring. European Journal of Inorganic Chemistry, 2008, 2008, 1497-1507.	2.0	6
72	First Stage of Thermal Aging under Oxidizing Conditions of a Ce _{0.62} Zr _{0.38} O ₂ Mixed Oxide with an Ordered Cationic Sublattice: A Chemical, Nanostructural, and Nanoanalytical Study. Chemistry of Materials, 2008, 20, 5107-5113.	6.7	37

#	Article	IF	CITATIONS
73	Some recent results on the correlation of nano-structural and redox properties in ceria-zirconia mixed oxides. Journal of Alloys and Compounds, 2008, 451, 521-525.	5.5	32
74	Preparation of Rhodium/Ce <i>_x</i> Pr ₁₋ <i>_x</i> O ₂ Catalysts:  A Nanostructural and Nanoanalytical Investigation of Surface Modifications by Transmission and Scanning-Transmission Electron Microscopy. Journal of Physical Chemistry C, 2008, 112, 5900-5910.	3.1	11
75	3D characterization and metrology of nanostructures by electron tomography. Microscopy and Microanalysis, 2008, 14, 284-285.	0.4	1
76	Electron tomography using compositional-sensitive diffraction contrast for 3D characterization of self-assembled semiconductor quantum dots. Microscopy and Microanalysis, 2008, 14, 1052-1053.	0.4	0
77	Structural Surface Investigations of Ceriumâ^'Zirconium Mixed Oxide Nanocrystals with Enhanced Reducibility. Journal of Physical Chemistry C, 2007, 111, 9001-9004.	3.1	36
78	Sizeâ€Controlled Waterâ€Soluble Ag Nanoparticles. European Journal of Inorganic Chemistry, 2007, 2007, 4823-4826.	2.0	41
79	Redox Behavior of Thermally Aged Ceriaâ^'Zirconia Mixed Oxides. Role of Their Surface and Bulk Structural Properties. Chemistry of Materials, 2006, 18, 2750-2757.	6.7	63
80	TEM Investigation of the Synthesis of Rh/CePrOx Catalysts. Microscopy and Microanalysis, 2006, 12, 760-761.	0.4	1
81	TEM (HREM) and STEM (HAADF/EDS) Study of the Metallic Dispersion in Supported Ruthenium Catalysts. Microscopy and Microanalysis, 2006, 12, 810-811.	0.4	0
82	Combined HREM and HAADF Scanning Transmission Electron Microscopy:Â A Powerful Tool for Investigating Structural Changes in Thermally Aged Ceriaâ^'Zirconia Mixed Oxides. Chemistry of Materials, 2005, 17, 4282-4285.	6.7	35
83	Stability and kinetics of the acid-promoted decomposition of Cu(ii) complexes with hexaazacyclophanes: kinetic studies as a probe to detect changes in the coordination mode of the macrocycles. Dalton Transactions, 2004, , 94-103.	3.3	23
84	Hydrogen-ion driven molecular motions in Cu2+-complexes of a ditopic phenanthrolinophane ligand. Chemical Communications, 2003, , 3032-3033.	4.1	15